Supporting Information

Synthesis, Characterisation and Properties of Rare Earth Oxyselenides $A_4O_4Se_3$ (A = Eu, Gd, Tb, Dy, Ho, Er, Yb and Y)

Andrew J. Tuxworth, Chun-Hai Wang, John S.O. Evans*.

Department of Chemistry, University Science Site, Durham University, South Road, Durham, DH1 3LE, UK

Contents:

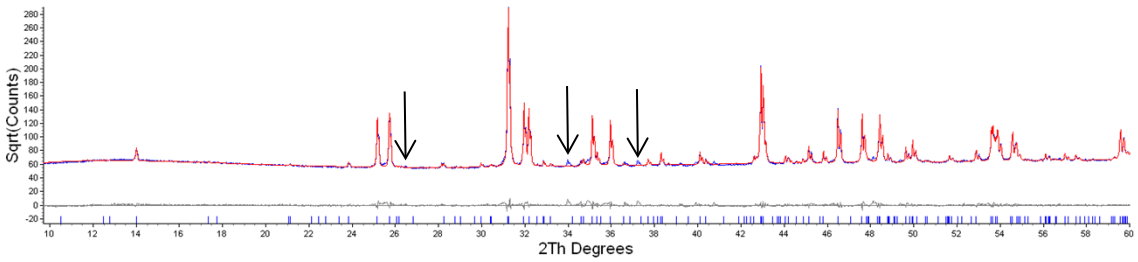

Figure SI1. Pawley refinement of $Eu_4O_4Se_3$ in *P*1 with a = 8.40408(7) Å, b = 3.90452(2) Å, c = 12.63857(7) Å, β = 91.3587(7)° ($\alpha = \gamma$ = 90°), R_{wp} = 2.939 %. Unindexed reflections marked by black arrows. Note square root counts scale to emphasise weak reflections.

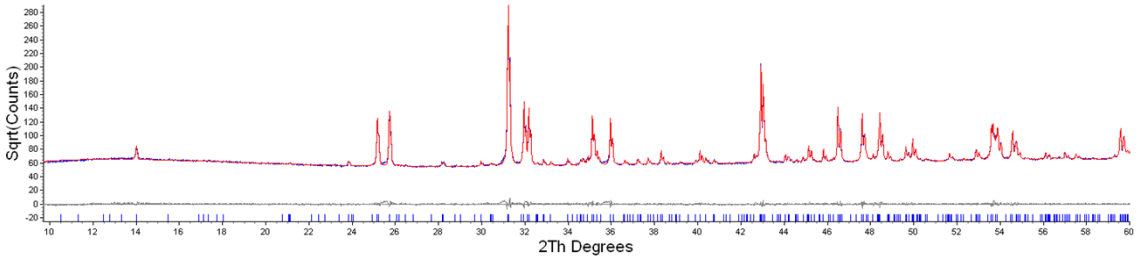

Figure SI2 Pawley refinement of $Eu_4O_4Se_3$ in P1 with a = 8.40437(8) Å, b = 7.80923(5) Å, c = 12.63876(7) Å, β = 91.3601(7)° ($\alpha = \gamma$ = 90°), R_{wp} = 2.362 %. Note square root counts scale. All unindexed reflections in Figure SI1 are predicted by the doubled *b*-axis cell.

Table SI1. Selected bond angles (°) for $Eu_4O_4Se_3$ $P2_1/c$ symmetry at 120 K.

Eu(2) - O(8) - Eu(2)	106.0(13)	Eu(1) - O(10) - Eu(2)	96.7(13)
Eu(2) - O(8) - Eu(3)	107.4(13)	Eu(1) - O(10) - Eu(4)	105.0(14)
Eu(2) - O(8) - Eu(3)	134.6(11)	Eu(2) - O(10) - Eu(4)	115.9(10)
Eu(2) - O(8) - Eu(4)	114.4(10)	Eu(2) - O(10) - Eu(4)	100.0(13)
Eu(2) - O(8) - Eu(4)	97.8(11)	Eu(1) - O(10) - Eu(4)	135.1(11)
Eu(3) - O(8) - Eu(4)	95.5(11)	Eu(4) - O(10) - Eu(4)	104.5(14)
Eu(1) - O(9) - Eu(1)	109.0(16)	Eu(1) - O(11) - Eu(2)	103.1(16)
Eu(1) - O(9) - Eu(3)	120.0(11)	Eu(1) - O(11) - Eu(3)	115.8(10)
Eu(1) - O(9) - Eu(3)	99.4(15)	Eu(2) - O(11) - Eu(3)	104.0(17)
Eu(1) - O(9) - Eu(4)	106.0(15)	Eu(1) - O(11) - Eu(3)	101.8(17)
Eu(1) - O(9) - Eu(4)	122.6(11)	Eu(2) - O(11) - Eu(3)	125.9(10)
Eu(3) - O(9) - Eu(4)	100.7(15)	Eu(3) - O(11) - Eu(3)	107.0(16)

Table SI2. Crystallographic data from Rietveld refinement of $Eu_4O_4Se_3$

	x	*y*	*z*	Occupancy	B_{iso} / Å^2
Eu1	0.11454(7)	0.3733(5)	0.40786(5)	1	0.44(1)
Eu2	0.37075(7)	0.1238(5)	0.58226(5)	1	0.42(1)
Eu3	0.11452(7)	-0.1243(5)	0.40900(5)	1	0.45(1)
Eu4	0.37168(7)	-0.3747(5)	0.57962(5)	1	0.48(1)
Se5	0.2316(1)	-0.6254(3)	0.73959(8)	1	0.90(1)
Se6	0.5243(1)	-0.6250(5)	0.74288(9)	1	0.86(1)
Se7	0.1233(1)	-0.1260(3)	0.72126(7)	1	0.86(1)
O8	0.3703(7)	-0.129(2)	0.4876(5)	1	0.06(1)
O9	0.1223(7)	-0.384(2)	0.4967(5)	1	0.06(14)
O10	0.3747(7)	-0.636(2)	0.4806(5)	1	0.06(14)
O11	0.1250(7)	0.107(1)	0.5032(5)	1	0.06(14)

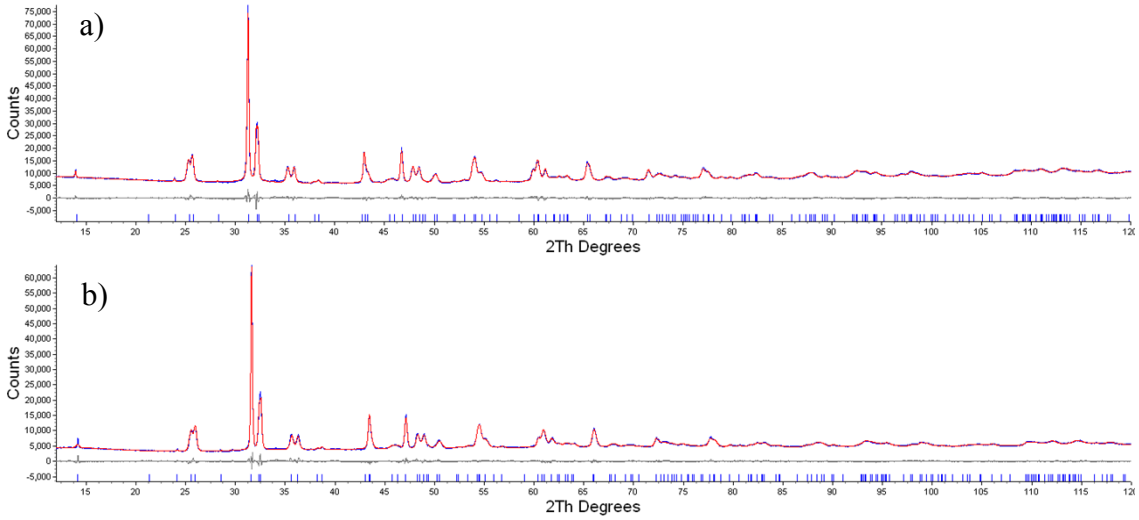

Figure SI3. Rietveld refinement profiles of X-ray powder diffraction data of a) $Gd_4O_4Se_3$ and b) $Tb_4O_4Se_3$ at room temperature, A2/m symmetry.

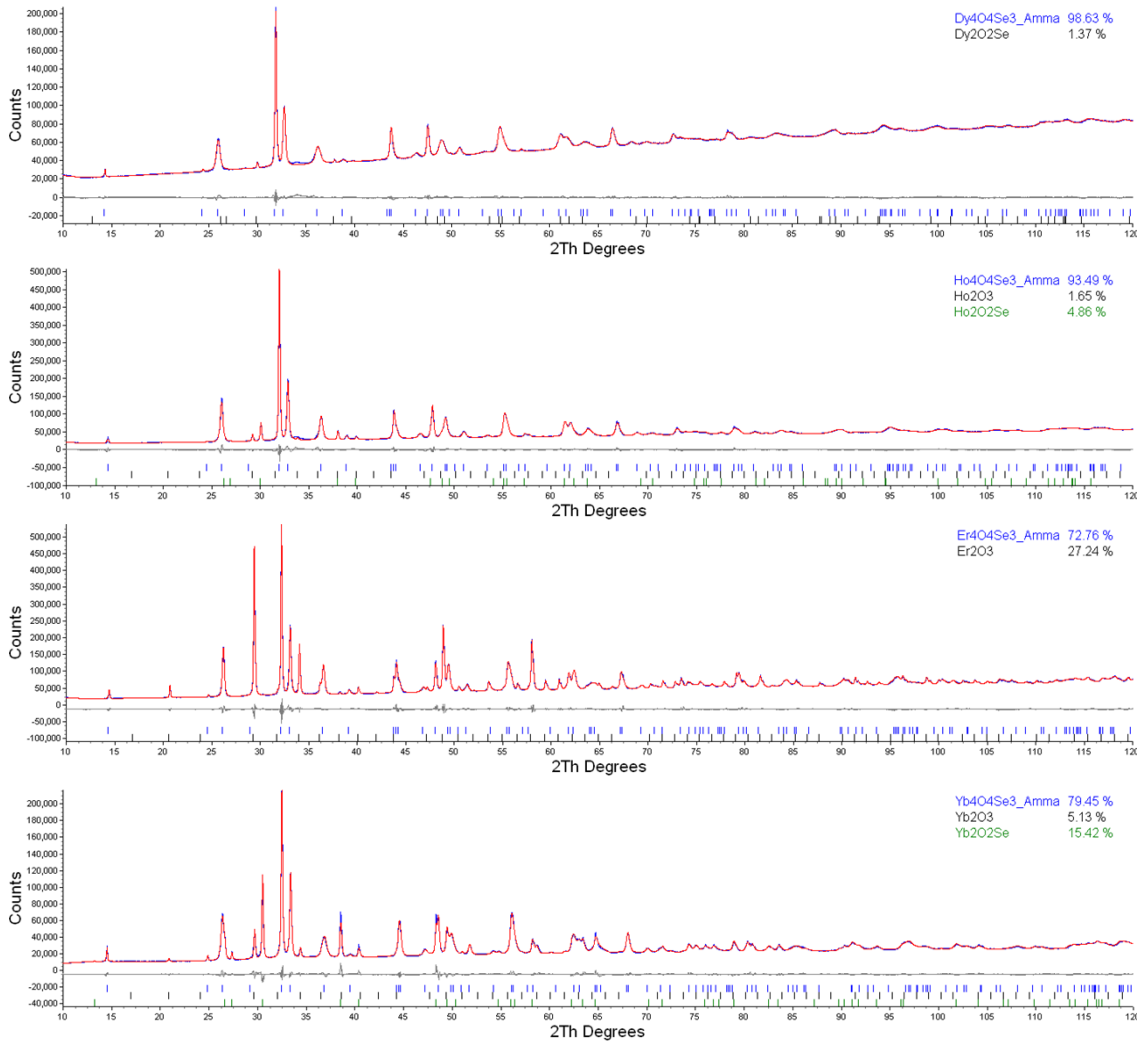

Figure SI4. Rietveld refinement profiles of δ-$A_4O_4Se_3$ powder X-ray diffraction data at room temperature, a) $Dy_4O_4Se_3$, b) $Ho_4O_4Se_3$, c) $Er_4O_4Se_3$ and d) $Yb_4O_4Se_3$. Blue vertical tick marks correspond to the calculated peak positions of $A_4O_4Se_3$ phase.

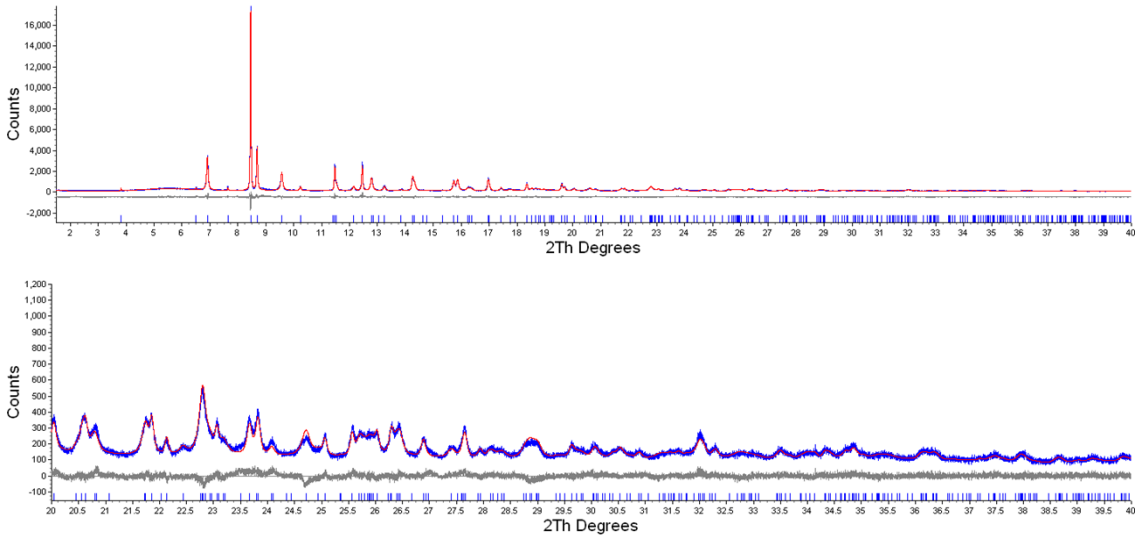

Figure SI5. Rietveld refinement profile of $Y_4O_4Se_3$, 11bmb_8961 AJT195, Amma symmetry, a = 4.12056(6) Å, b = 3.81484(4) Å and c =12.4212(1) Å. R_{wp} = 8.629 %, R_p = 6.663, R_{Bragg} =2.866 %, gof = 1.488.

Temperature dependence of unit cell parameters for $Nd_4O_4Se_3$.

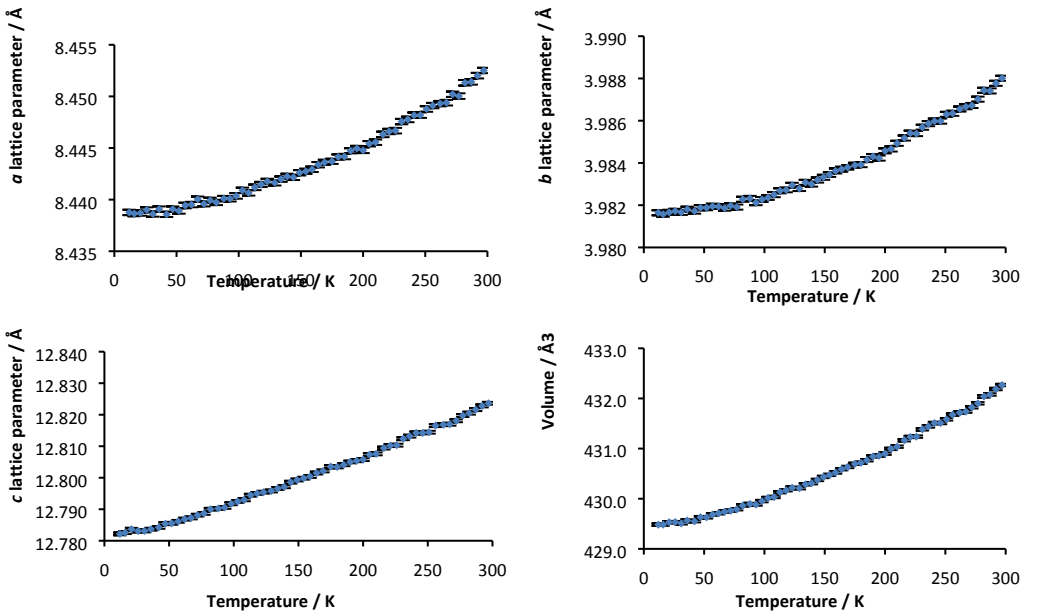

Temperature dependence of unit cell parameters for $Sm_4O_4Se_3$.

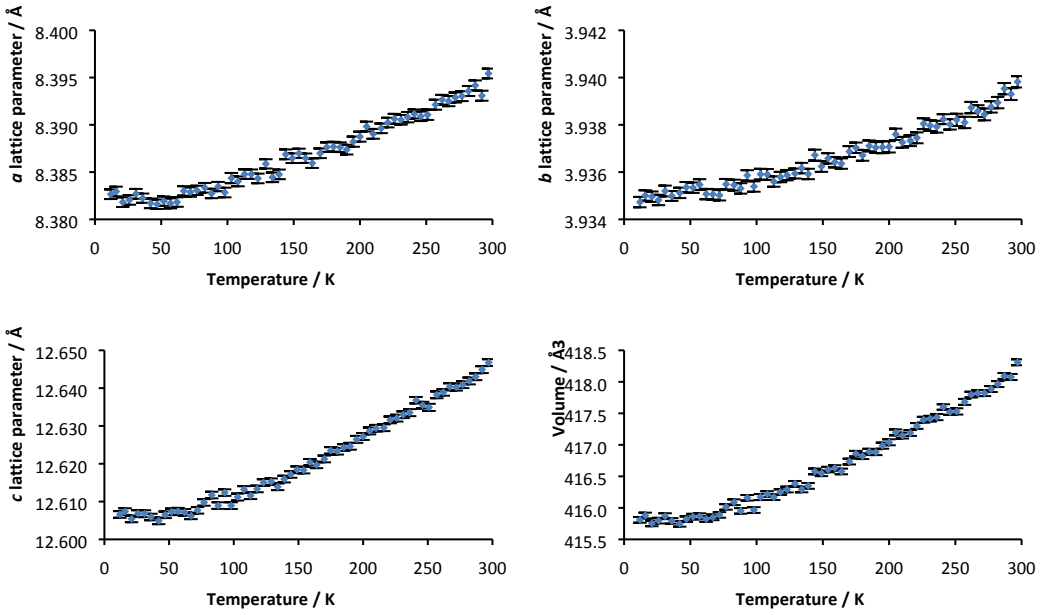

Temperature dependence of unit cell parameters for $Eu_4O_4Se_3$

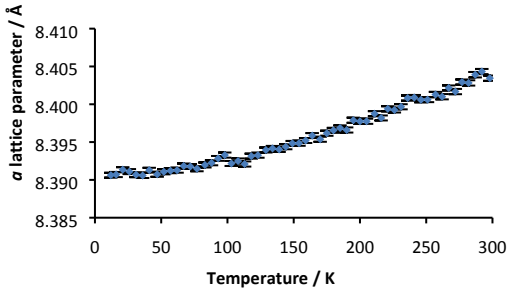

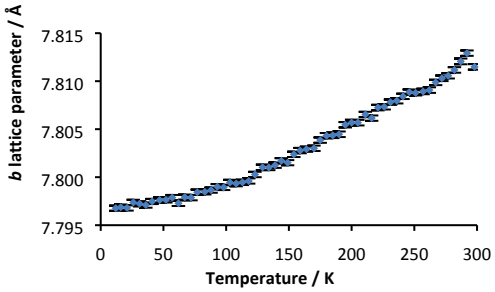

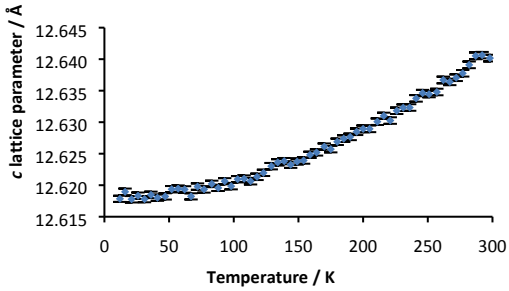

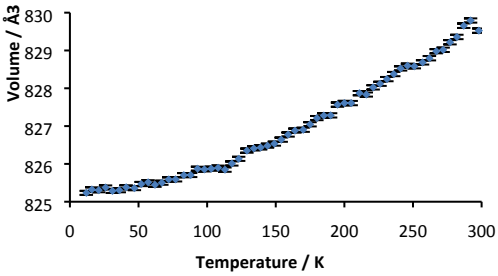

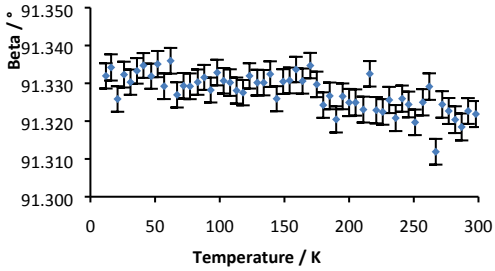

Temperature dependence of unit cell parameters for Gd4O4Se3.

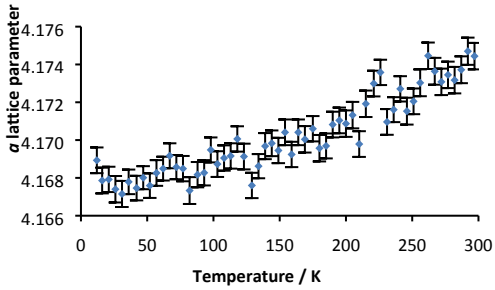

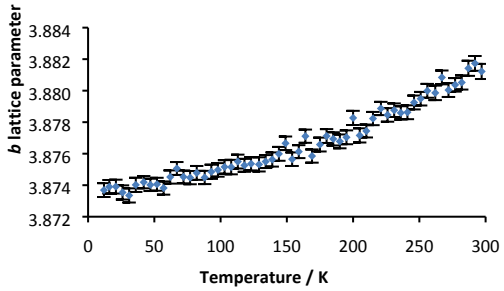

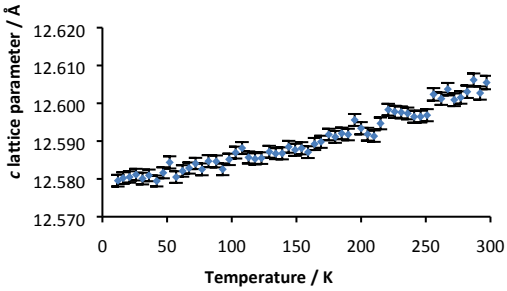

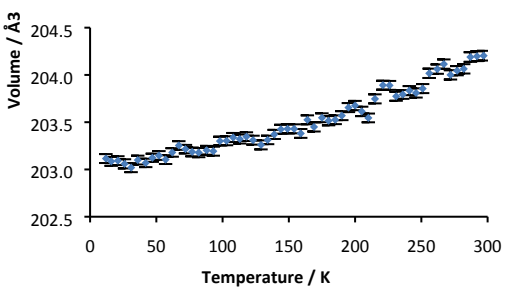

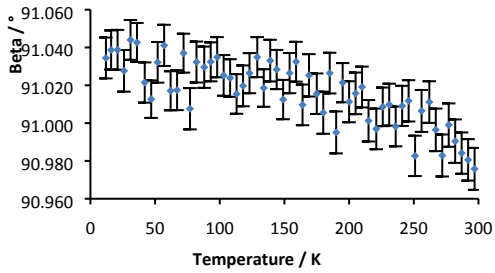

Temperature dependence of unit cell parameters for $Tb_4O_4Se_3$.

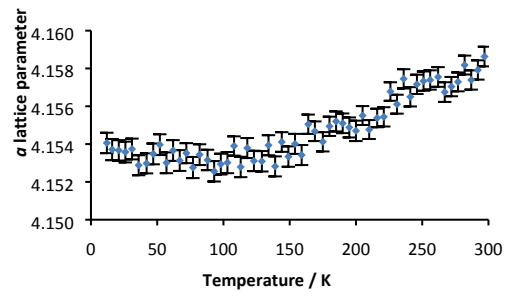

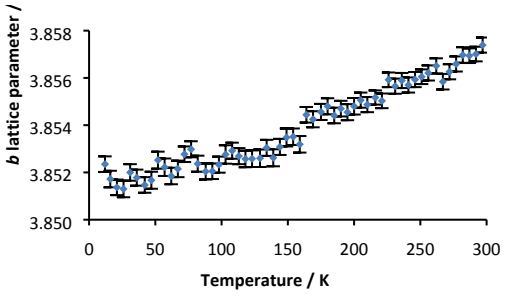

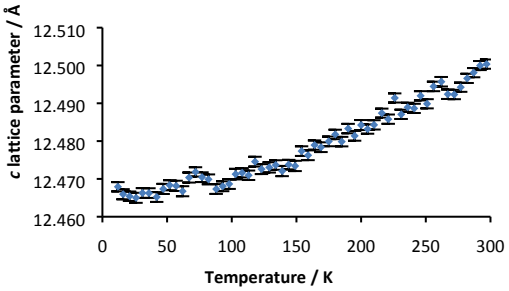

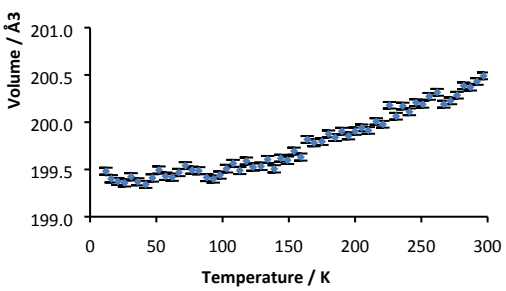

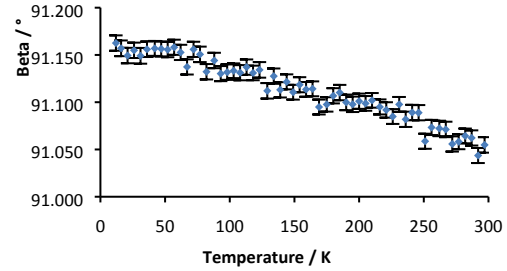

Temperature dependence of unit cell parameters for $Dy_4O_4Se_3$.

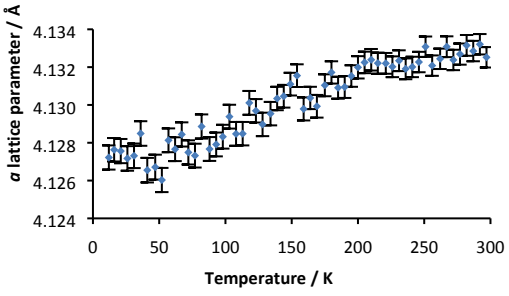

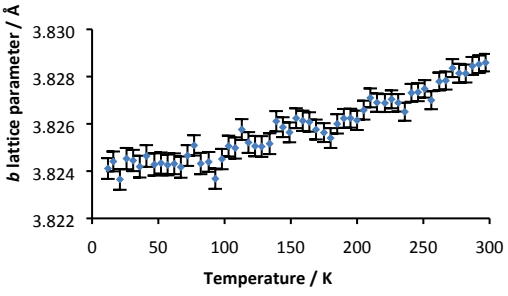

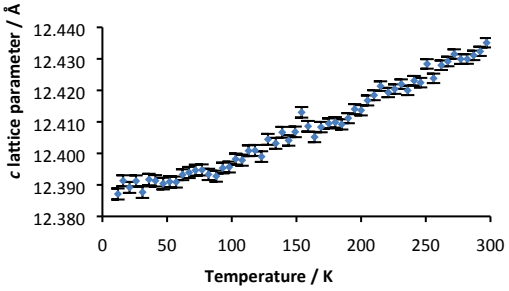

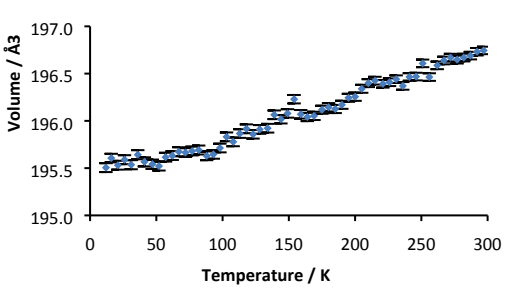

Temperature dependence of unit cell parameters for $Ho_4O_4Se_3$.

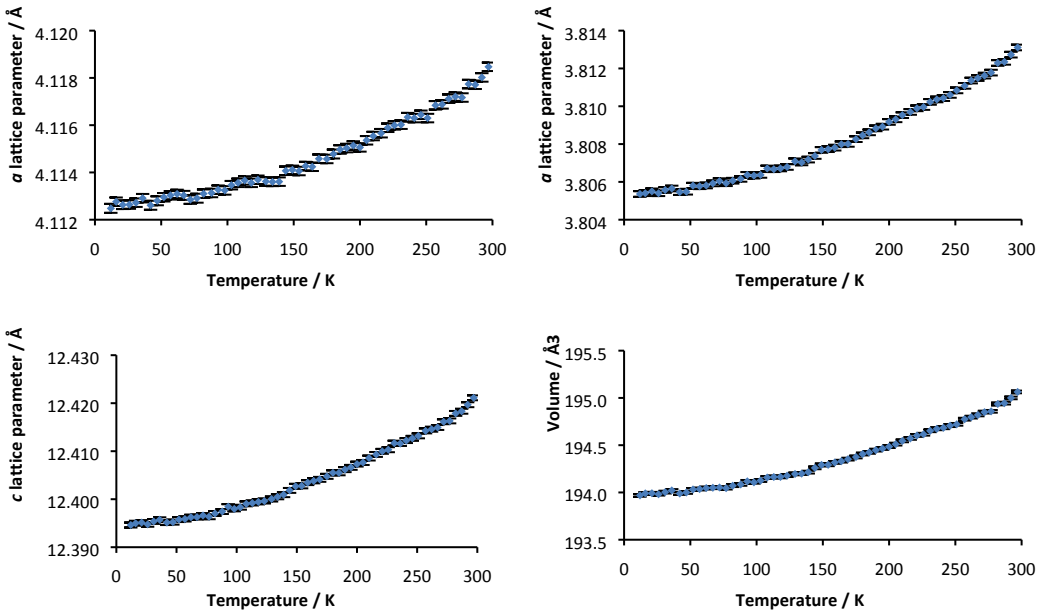

Temperature dependence of unit cell parameters for $Er_4O_4Se_3$.

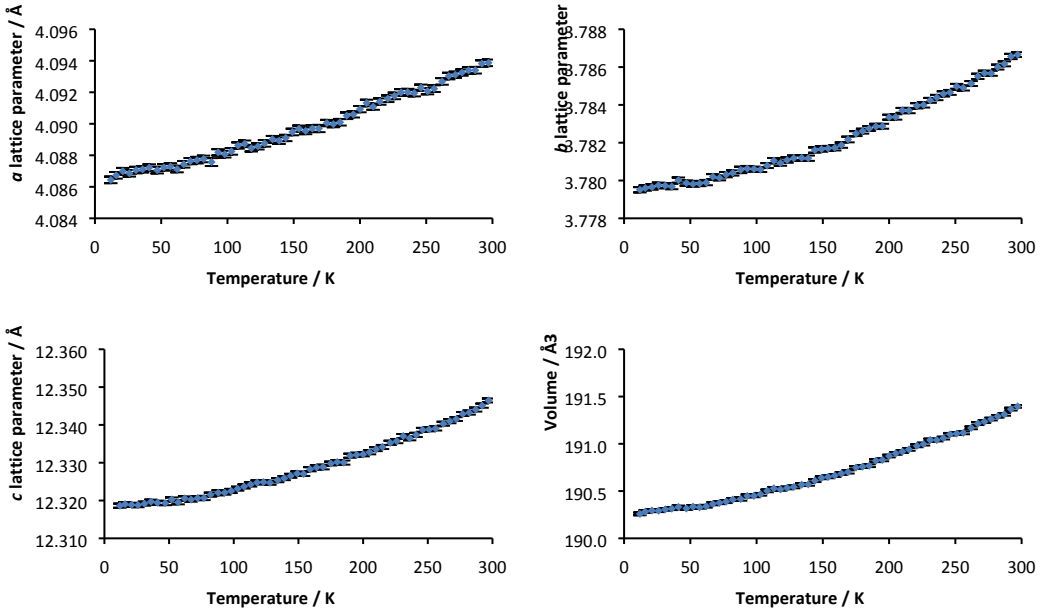

Temperature dependence of unit cell parameters for $Y_4O_4Se_3$.

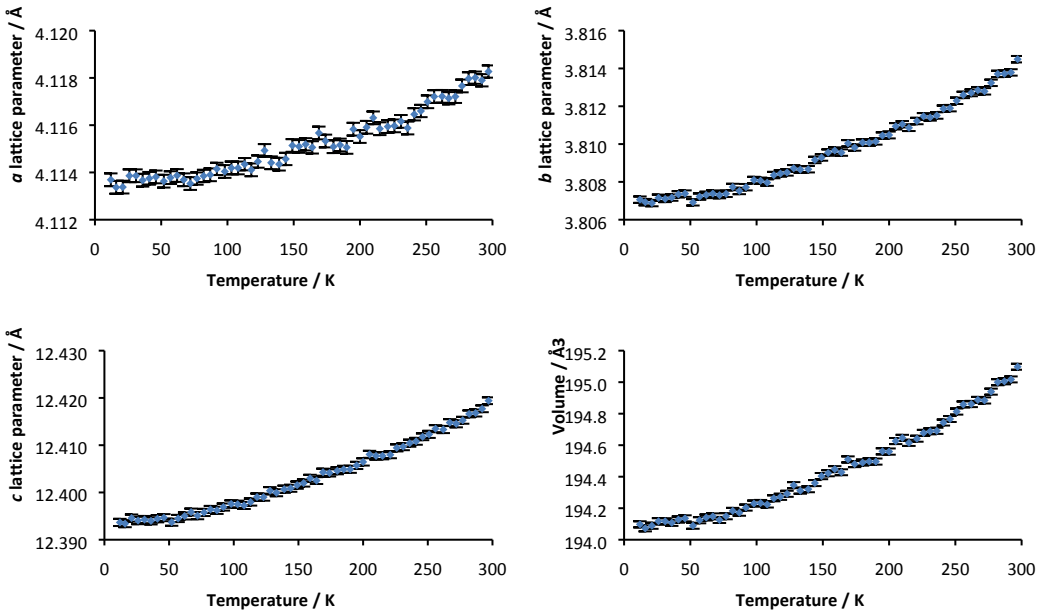

Figure SI6. Unit cell parameters derived from variable temperature powder X-ray diffraction for $A_4O_4Se_3$ materials. Sample labels given above each graph.

$Eu_4O_4Se_3$

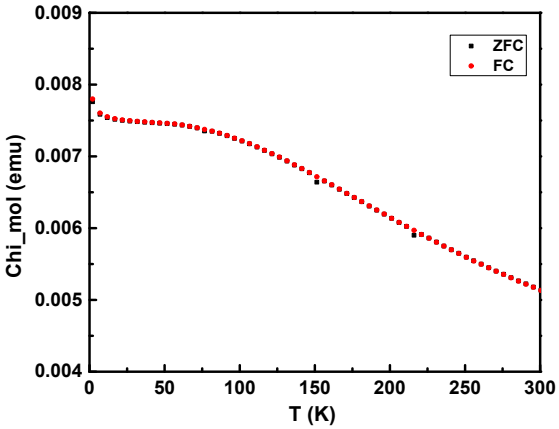
ZFC
FC
Chi_mol (emu)
T (K)
0.009
0.008
0.007
0.006
0.005
0.004
0
50
100
150
200
250
300

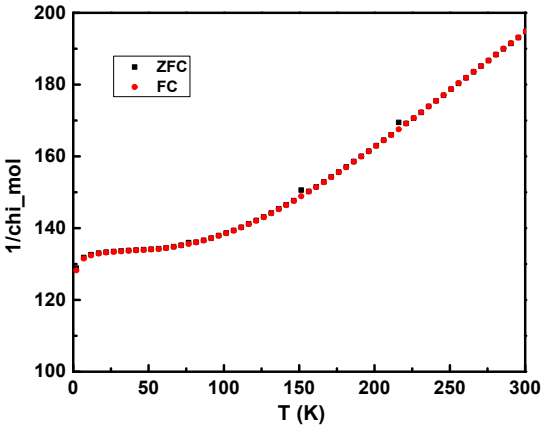
ZFC
FC
1/chi_mol
T (K)
200
180
160
140
120
100
0
50
100
150
200
250
300

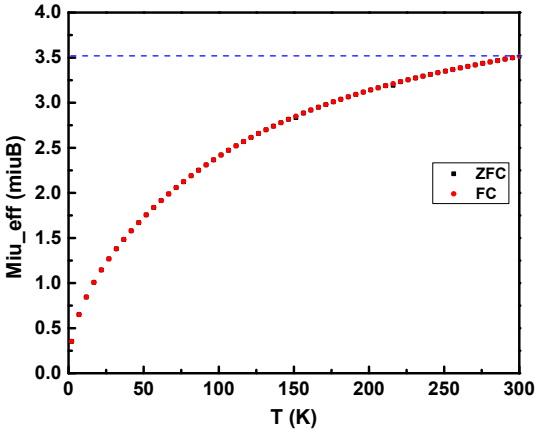
ZFC
FC
Miu_eff (miuB)
T (K)
4.0
3.5
3.0
2.5
2.0
1.5
1.0
0.5
0.0
0
50
100
150
200
250
300

$Gd_4O_4Se_3$

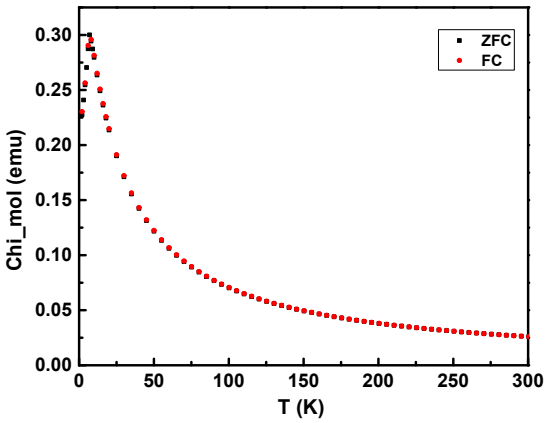
ZFC
FC
Chi_mol (emu)
T (K)

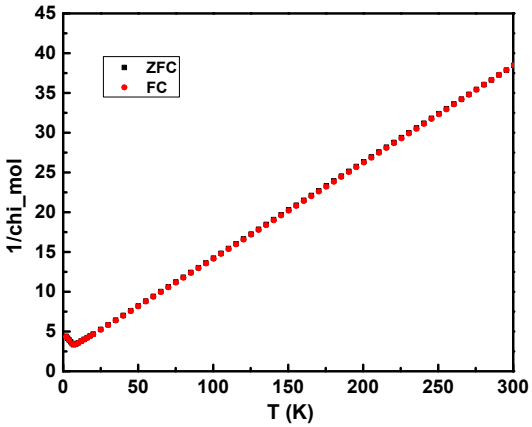
ZFC
FC
1/chi_mol
T (K)

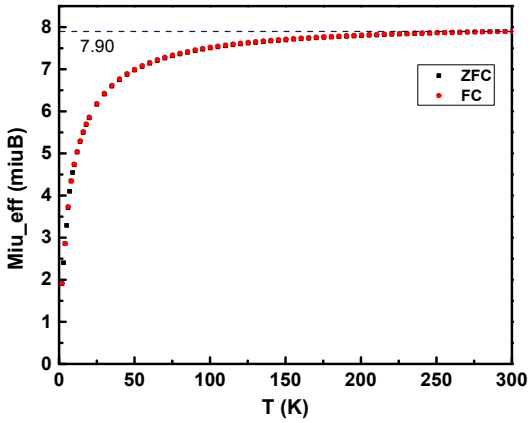
7.90
ZFC
FC
Miu_eff (miuB)
T (K)

$Dy_4O_4Se_3$

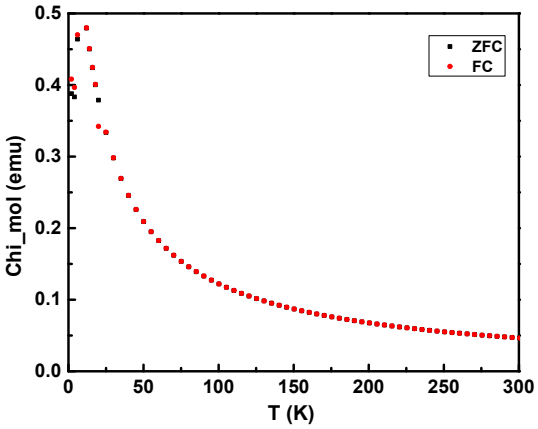
ZFC
FC
Chi_mol (emu)
T (K)

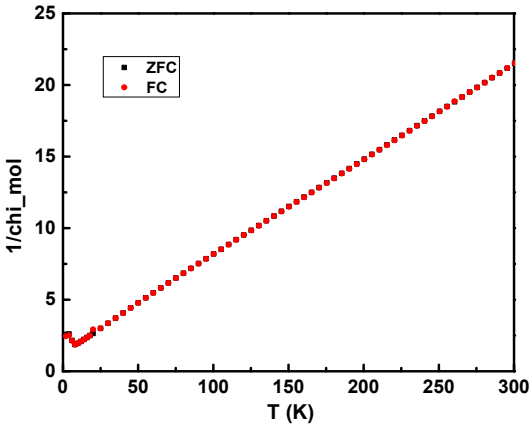
ZFC
FC
1/chi_mol
T (K)

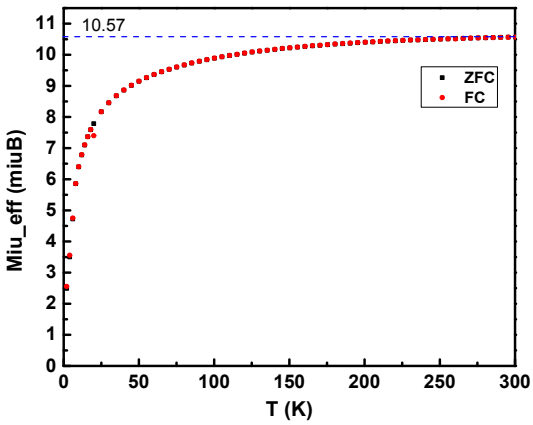
10.57
ZFC
FC
Miu_eff (miuB)
T (K)

$Tb_4O_4Se_3$

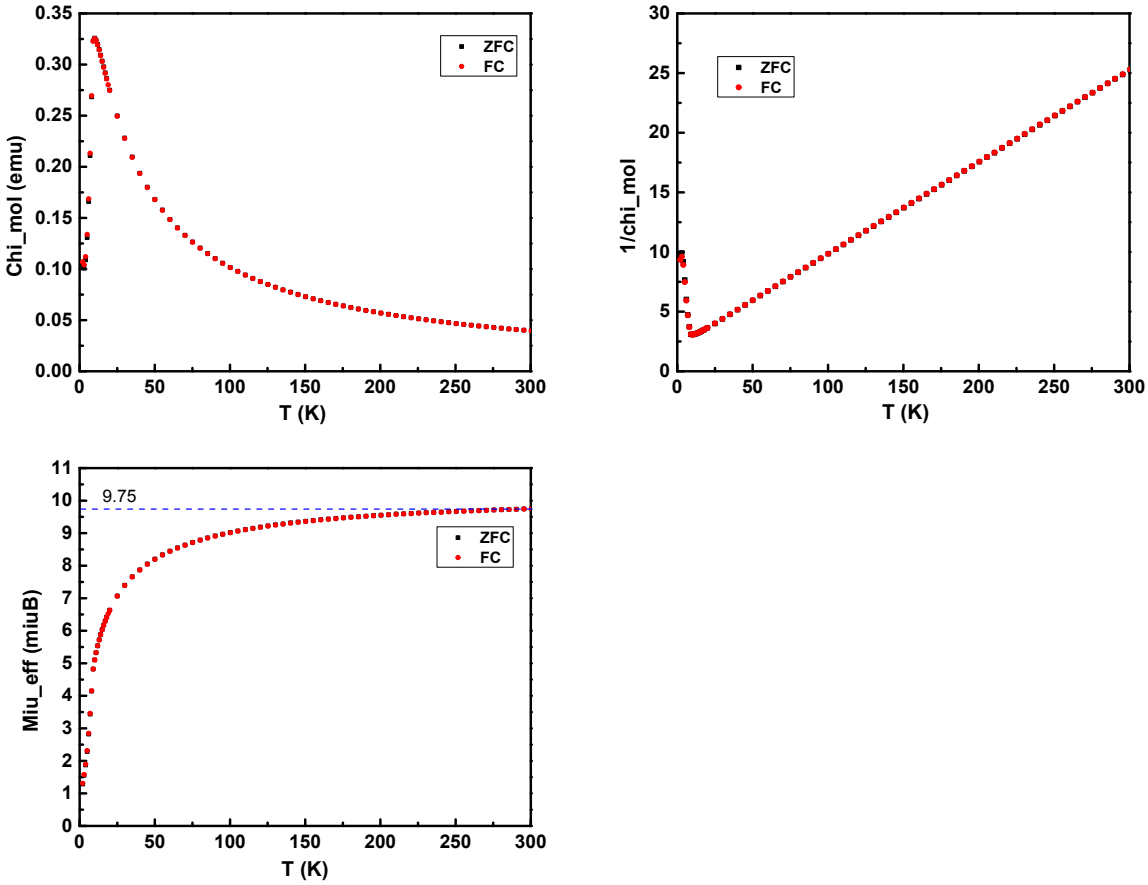

Figure SI7. Magnetic data for $A_4O_4Se_3$ materials. For each material field cooled and zero-field cooled susceptibility, $1/\chi_{mol}$ vs T and μ_{eff} are plotted. Sample labels given above each graph.

$Eu_4O_4Se_3$

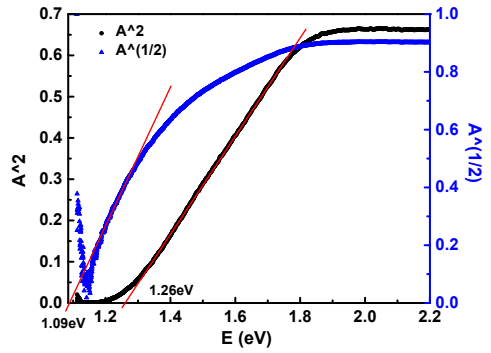

$Gd_4O_4Se_3$

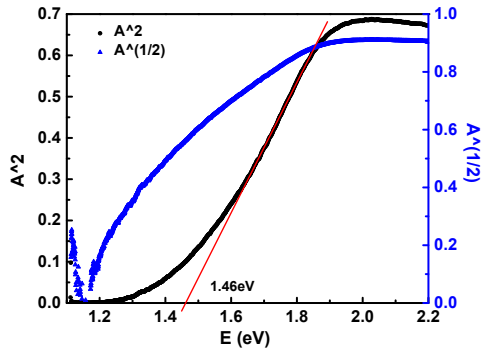

$Tb_4O_4Se_3$

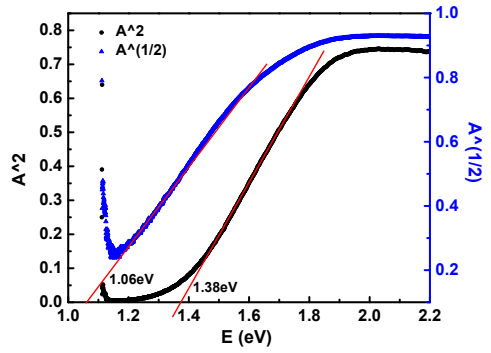

$Dy_4O_4Se_3$

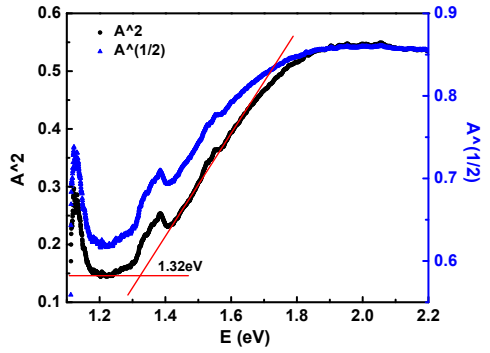

$Ho_4O_4Se_3$

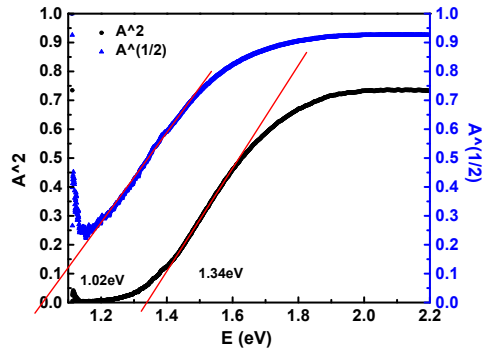

$Er_4O_4Se_3$

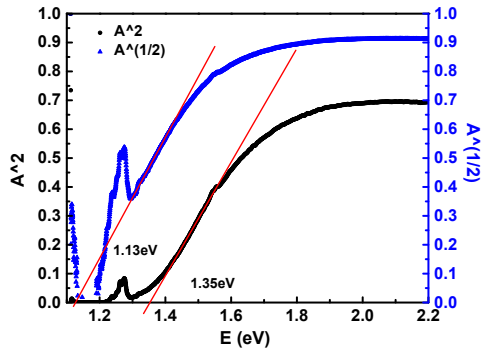

$Yb_4O_4Se_3$

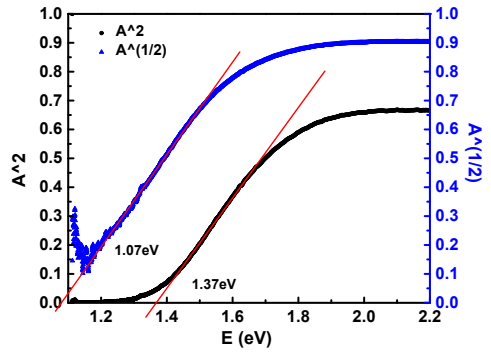

$Y_4O_4Se_3$

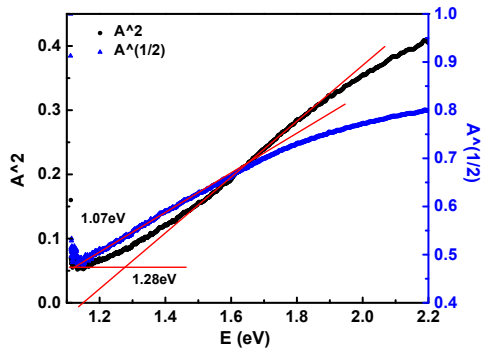

Figure SI8. Absorption curves for $A_4O_4Se_3$ samples. Blue: A - $E^{1/2}$, Black: A - E^2.

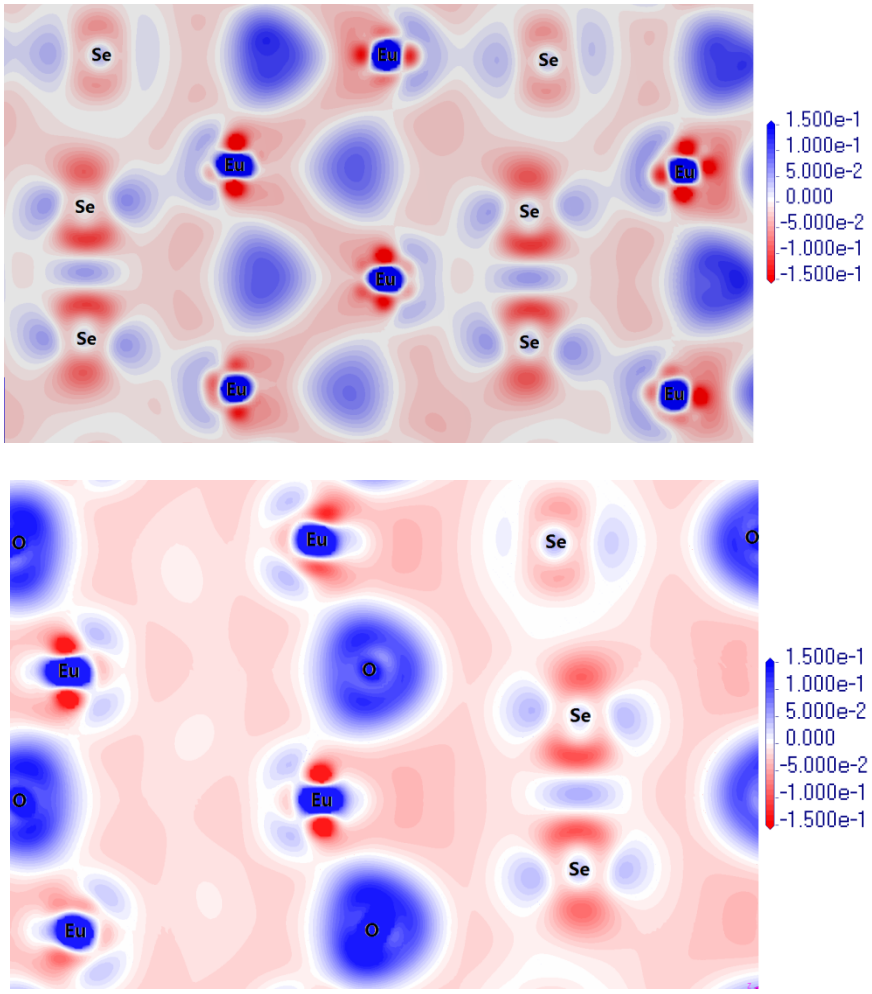

Figure SI9. Electron density difference (two difference cross sections) between free atoms and the atoms in $Eu_4O_4Se_3$ from DFT calculations.

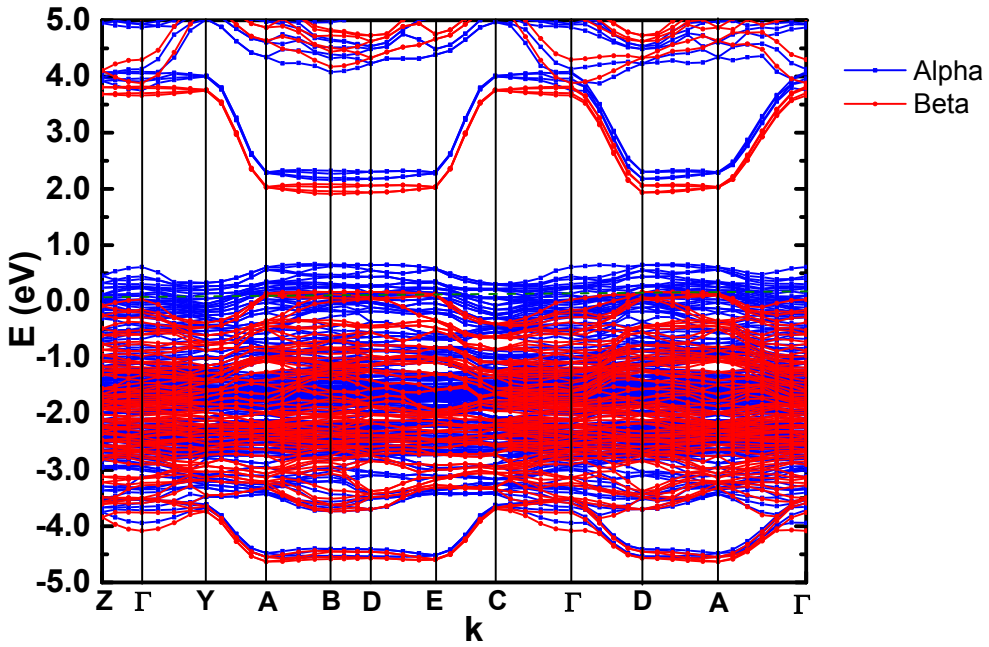

Figure SI10. Band structure of $Eu_4O_4Se_3$ from DFT calculations. The Fermi level is set as $E = 0$ eV. Alpha and beta indicate the spin up and spin down bands respectively.

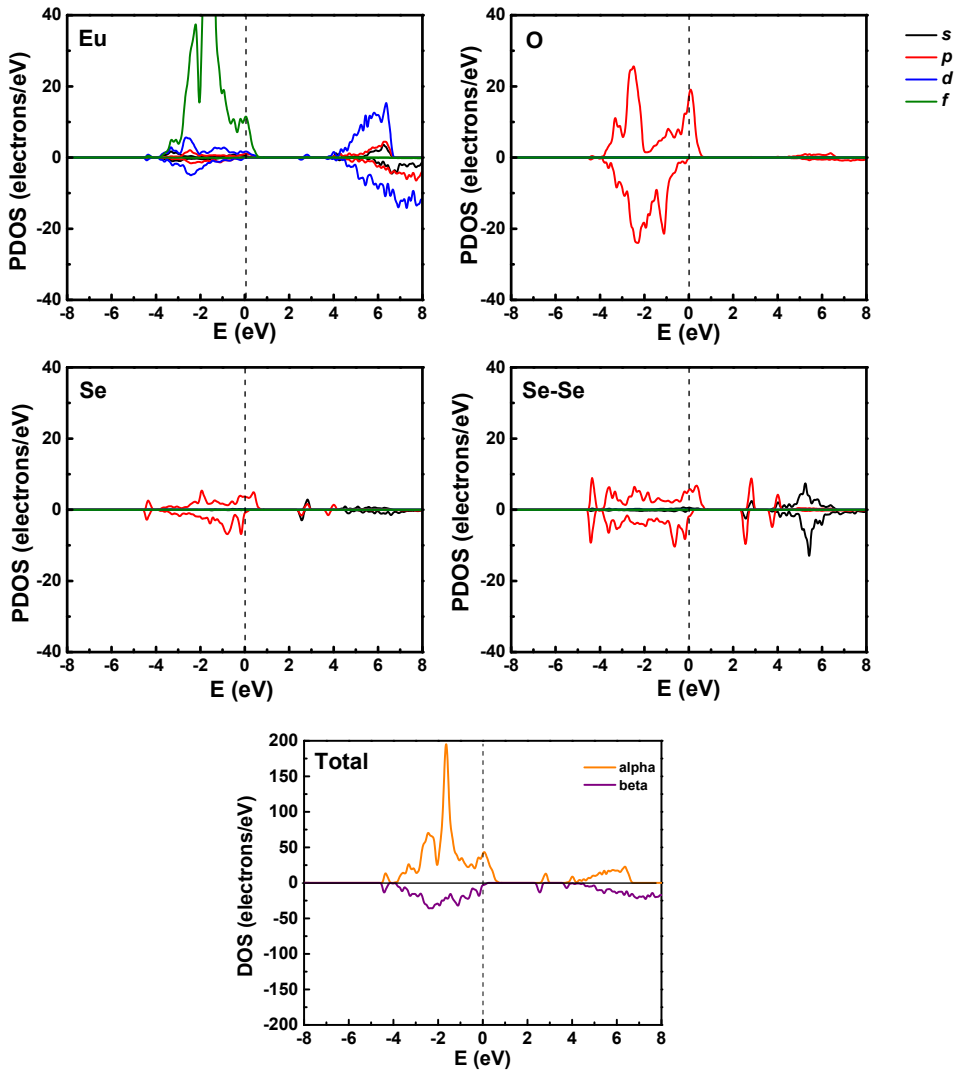

Figure SI11. Partial density of state (PDOS) of different atoms and total DOS of $Eu_4O_4Se_3$. The Fermi level is set as $E = 0$ eV. Se and Se-Se indicates the Se^{2-} and Se_2^{2-} in the structure. PDOS of spin up (alpha) and spin down electrons (orbitals) are shown in the positive and negative PDOS quadrant.